

Scalar-tensor cosmologies: fixed points of the Jordan frame scalar field

Laur Järv,^{1a} Piret Kuusk,^{2a} and Margus Saal^{3b}

^a *Institute of Physics, University of Tartu, Riia 142, Tartu 51014, Estonia*

^b *Tartu Observatory, Tõravere 61602, Estonia*

Abstract

We study the evolution of homogeneous and isotropic, flat cosmological models within the general scalar-tensor theory of gravity with arbitrary coupling function and potential. After introducing the limit of general relativity we describe the details of the phase space geometry. Using the methods of dynamical systems for the decoupled equation of the Jordan frame scalar field we find the fixed points of flows in two cases: potential domination and matter domination. We present the conditions on the mathematical form of the coupling function and potential which determine the nature of the fixed points (attractor or other). There are two types of fixed points, both are characterized by cosmological evolution mimicking general relativity, but only one of the types is compatible with the Solar System PPN constraints. The phase space structure should also carry over to the Einstein frame as long as the transformation between the frames is regular which however is not the case for the latter (PPN compatible) fixed point.

PACS: 98.80.Jk, 04.50.+h, 04.40.Nr

¹ Electronic address: laur@fi.tartu.ee

² Electronic address: piret@fi.tartu.ee

³ Electronic address: margus@fi.tartu.ee

1 Introduction

Scalar-tensor theories (STT) of gravitation [1, 2, 3] have emerged in different contexts of theoretical physics, e.g. in Kaluza-Klein type unifications, supergravity, and low energy approximations of string theories. The scalar-tensor action functional has been also used in topology as a mathematical tool for solving the geometrization conjecture of 3-manifolds via the Ricci flow [4].

In cosmology STT has been invoked to model the accelerated expansion of inflation [5] and dark energy [6] (for some recent papers see e.g. Ref. [7]). However, observations in the Solar System tend to indicate that in the intermediate-range distances the present Universe around us is successfully described by the Einstein tensorial gravity alone [8]. This means that only such models of scalar-tensor gravity are viable which in their late time cosmological evolution imply local observational consequences very close to those of Einstein's general relativity (GR) [9].

The importance of the convergence of the STT solutions to those of GR at late times, guaranteeing agreement with the present post-Newtonian observations was recognized by Bekenstein and Meisels [10] already long ago. Damour and Nordtvedt [11, 12] argued that for a wide class of homogeneous and isotropic scalar-tensor cosmological models there exists an attractor mechanism taking them to the limit of the corresponding general relativistic models. In subsequent papers the issue has been pursued by various approaches [13, 14, 15, 16].

The methods of dynamical systems provide natural tools to analyze the problem. Most previous studies which have considered STT cosmology as a dynamical system have focused upon examples with specific coupling functions, see Refs. [17, 18, 19, 20] for works based on the Einstein frame and Refs. [21, 22, 23, 24, 20] for the Jordan frame. In the Jordan frame the main properties of the general phase space geometry were outlined by Faraoni [25], while Refs. [26, 27] consider general Jordan frame dynamics with particular attention to the de Sitter fixed point.

Although the equations of motion in the Einstein frame may have a simpler form, the cosmological observations are easier to interpret in the Jordan frame where matter is minimally coupled. In general there is a one-to-one correspondence between the phase spaces in the two conformal frames [28, 29, 3, 30, 31], provided that the transformations from one frame to another are regular. However, as it was pointed out in Ref. [20], the differential equation relating the scalar fields in these two frames becomes singular at the limit of general relativity. Therefore utmost care must be exercised when addressing the question whether general relativity is an attractor, as the answer may depend on the frame chosen.

In this paper we take the Jordan frame and consider general scalar-tensor theories which contain two functional degrees of freedom, the coupling function $\omega(\Psi)$ and the scalar potential $V(\Psi)$. We perform the dynamical systems analysis for the flat Friedmann-Lemaître-Robertson-

Walker (FLRW) backgrounds with ideal barotropic fluid matter. Our strategy is to find the fixed points for the scalar field dynamics and compare these with the conditions of the limit of general relativity in the Solar System, as established by the parameterized post-Newtonian (PPN) formalism. Therefore, if the functional forms of $\omega(\Psi)$ and $V(\Psi)$ are specified from some considerations (e.g. the compactification manifold), our results allow to determine the fixed points along with their type and thus immediately decide whether general relativity is an attractor, i.e. whether the model at hand is viable or not.

The plan of the paper is the following. In section 2 we write the field equations as a dynamical system and find the conditions which reduce these equations to the FLRW equations of general relativity (possibly with a cosmological constant), concluding that these conditions are marginally stricter than the standard PPN conditions. In section 3 we describe the general phase space and its physical subspace determined by the Friedmann constraint equation. In section 4 we consider the case of potential domination with (effectively) vanishing matter density, find the fixed points and determine their properties. For investigating the case of matter domination (with vanishing scalar potential) in section 5, we follow Refs. [12] and [15] to introduce a new time parameter which allows us derive a decoupled “master” equation for the scalar field and again perform the fixed point analysis. In section 5 we briefly discuss comparison to some previous works and end with a speculation about the possible relevance of our results for the moduli stabilization problem in string theory. Section 6 gives a summary.

2 Scalar-tensor cosmology as a dynamical system and the limit of general relativity

We consider a general scalar-tensor theory in the Jordan frame given by the action functional

$$S = \frac{1}{2\kappa^2} \int d^4x \sqrt{-g} \left[\Psi R(g) - \frac{\omega(\Psi)}{\Psi} \nabla^\rho \Psi \nabla_\rho \Psi - 2\kappa^2 V(\Psi) \right] + S_m(g_{\mu\nu}, \chi_m). \quad (1)$$

Here $\omega(\Psi)$ is a coupling function and $V(\Psi)$ is a scalar potential, ∇_μ denotes the covariant derivative with respect to the metric $g_{\mu\nu}$, $\kappa^2 = 8\pi G_N$, and S_m is the matter part of the action as all other fields are included in χ_m . In order to keep the effective Newtonian gravitational constant positive [34, 14] we assume that $0 < \Psi < \infty$.

The field equations for the flat ($k = 0$) FLRW line element and perfect barotropic fluid matter, $p = w\rho$, read

$$H^2 = -H \frac{\dot{\Psi}}{\Psi} + \frac{1}{6} \frac{\dot{\Psi}^2}{\Psi^2} \omega(\Psi) + \frac{\kappa^2}{3} \frac{\rho}{\Psi} + \frac{\kappa^2}{3} \frac{V(\Psi)}{\Psi}, \quad (2)$$

$$2\dot{H} + 3H^2 = -2H \frac{\dot{\Psi}}{\Psi} - \frac{1}{2} \frac{\dot{\Psi}^2}{\Psi^2} \omega(\Psi) - \frac{\ddot{\Psi}}{\Psi} - \frac{\kappa^2}{\Psi} w\rho + \frac{\kappa^2}{\Psi} V(\Psi), \quad (3)$$

$$\begin{aligned} \ddot{\Psi} = & -3H\dot{\Psi} - \frac{1}{2\omega(\Psi) + 3} \frac{d\omega(\Psi)}{d\Psi} \dot{\Psi}^2 + \frac{\kappa^2}{2\omega(\Psi) + 3} (1 - 3w) \rho \\ & + \frac{2\kappa^2}{2\omega(\Psi) + 3} \left[2V(\Psi) - \Psi \frac{dV(\Psi)}{d\Psi} \right], \end{aligned} \quad (4)$$

$H \equiv \dot{a}/a$. The matter conservation law is the usual

$$\dot{\rho} + 3H (w + 1) \rho = 0 \quad (5)$$

and we assume $\rho \geq 0$. Eqs. (2)–(5) are too cumbersome to be solved analytically, but useful information about the general characteristics of solutions can be obtained by rewriting (2)–(5) in the form of a dynamical system and finding the fixed points which describe the asymptotic behaviour of solutions.

The phase space of the system is spanned by four variables $\{\Psi, \dot{\Psi}, H, \rho\}$. Defining $\Psi \equiv x$, $\dot{\Psi} \equiv y$ the dynamical system corresponding to equations (2)–(5) can be written as follows:

$$\dot{x} = y, \quad (6)$$

$$\dot{y} = -\frac{1}{2\omega(x) + 3} \left[\frac{d\omega(x)}{dx} y^2 - \kappa^2 (1 - 3w) \rho + 2\kappa^2 \left(\frac{dV(x)}{dx} x - 2V(x) \right) \right] - 3Hy, \quad (7)$$

$$\begin{aligned} \dot{H} = & \frac{1}{2x(2\omega(x) + 3)} \left[\frac{d\omega(x)}{dx} y^2 - \kappa^2 (1 - 3w) \rho + 2\kappa^2 \left(\frac{dV(x)}{dx} x - 2V(x) \right) \right] \\ & - \frac{1}{2x} \left[6H^2 x + 2Hy - \kappa^2 (1 - w) \rho - 2\kappa^2 V(x) \right], \end{aligned} \quad (8)$$

$$\dot{\rho} = -3H(1 + w)\rho. \quad (9)$$

Based on these equations we may make a couple of quick qualitative observations about some general features of the solutions. For example, the limit $\Psi \rightarrow 0$ in general implies $|\dot{H}| \rightarrow \infty$, hence the solutions can not safely pass from positive to negative values of Ψ (from “attractive” to “repulsive” gravity), but hit a space-time singularity as the curvature invariants diverge. Similarly, the limit $2\omega + 3 \rightarrow 0$ implies $|\dot{H}| \rightarrow \infty$ with the same conclusion that passing through $\omega(\Psi) = -\frac{3}{2}$ (corresponding to the change of the sign of the scalar field kinetic term in the Einstein frame action) would entail a space-time singularity and is impossible. (Let us remark here, that these observations are quite general and do not preclude specially fine-tuned solutions in some fine-tuned models which may remain regular while crossing these points, like in Ref. [22].)

The limit $\frac{1}{2\omega+3} \rightarrow 0$ deserves a more closer examination. Let us define x_* by

$$\frac{1}{2\omega(x_*) + 3} = 0. \quad (10)$$

Expressing H from the Friedmann constraint (2),

$$H = -\frac{y}{2x} \left(\frac{+}{-} \right) \sqrt{(2\omega(x) + 3) \frac{y^2}{12x^2} + \frac{\kappa^2(\rho + V(x))}{3x}}, \quad (11)$$

makes clear that $|H|$ diverges as $x \rightarrow x_*$, unless also $y \rightarrow 0$ at the same time. What happens in the latter case is determined by the first term under the square root above. We can compute its limit by Taylor expanding

$$\begin{aligned}
\lim_{\substack{y \rightarrow 0 \\ x \rightarrow x_*}} (2\omega(x) + 3)y^2 &= \lim_{\substack{\Delta y \rightarrow 0 \\ \Delta x \rightarrow 0}} \frac{y^2|_{y=0} + 2y|_{y=0}\Delta y + (\Delta y)^2}{\frac{1}{2\omega(x)+3}\Big|_{x=x_*} + \frac{d}{dx}\left(\frac{1}{2\omega(x)+3}\right)\Big|_{x=x_*}\Delta x + \frac{1}{2}\frac{d^2}{dx^2}\left(\frac{1}{2\omega(x)+3}\right)\Big|_{x=x_*}(\Delta x)^2 + \dots} \\
&= \lim_{r \rightarrow 0} \frac{r^2 \sin^2 \theta}{\frac{d}{dx}\left(\frac{1}{2\omega(x)+3}\right)\Big|_{x=x_*} r \cos \theta + \frac{1}{2}\frac{d^2}{dx^2}\left(\frac{1}{2\omega(x)+3}\right)\Big|_{x=x_*} r^2 \cos^2 \theta + \dots} \\
&\begin{cases} = 0, & \text{if } \frac{d}{dx}\left(\frac{1}{2\omega(x)+3}\right)\Big|_{x=x_*} \neq 0, \\ \sim \tan^2 \theta, & \text{if } \frac{d}{dx}\left(\frac{1}{2\omega(x)+3}\right)\Big|_{x=x_*} = 0, \quad \frac{d^2}{dx^2}\left(\frac{1}{2\omega(x)+3}\right)\Big|_{x=x_*} \neq 0, \\ = \infty, & \text{if } \frac{d}{dx}\left(\frac{1}{2\omega(x)+3}\right)\Big|_{x=x_*} = 0, \quad \frac{d^2}{dx^2}\left(\frac{1}{2\omega(x)+3}\right)\Big|_{x=x_*} = 0, \end{cases} \quad (12)
\end{aligned}$$

where $\Delta x = r \cos \theta$, $\Delta y = r \sin \theta$ was taken. (We have neglected the unphysical direction $|\theta| = \frac{\pi}{2}$ that corresponds to approaching the point $(x = x_*, y = 0)$ along the line $x = x_*$ where $|H|$ is divergent.) So, in the limit $x \rightarrow x_*, y \rightarrow 0$ the value of H is determined by the lowest non-zero derivative of $\frac{1}{2\omega(x)+3}$. If the both the first and second derivative vanish, then $|H|$ diverges implying a spacetime singularity. If the first derivative vanishes but the second derivative is not zero,

$$\frac{d}{dx}\left(\frac{1}{2\omega(x)+3}\right)\Big|_{x=x_*} = 0, \quad \frac{d^2}{dx^2}\left(\frac{1}{2\omega(x)+3}\right)\Big|_{x=x_*} \neq 0, \quad (13)$$

then H is finite but (possibly) different for each solution as it depends on the angle of approach θ , while the Friedmann equation in this case acquires an extra term when compared to general relativity. If the first derivative is not zero,

$$\frac{d}{dx}\left(\frac{1}{2\omega(x)+3}\right)\Big|_{x=x_*} = \frac{1}{(2\omega(x_*)+3)^2} \frac{d\omega}{dx}\Big|_{x=x_*} \neq 0, \quad (14)$$

then H approaches the value $H_*^2 = \frac{\kappa^2}{3x_*}(\rho + V(x_*))$, mimicking the Friedmann equation of general relativity with $8\pi G = \frac{\kappa^2}{x_*}$ and $\Lambda = \frac{\kappa^2}{x_*}V(x_*)$.

To summarize, we have just observed that in the limit (a) $\frac{1}{2\omega(x)+3} \rightarrow 0$, (b) $y \rightarrow 0$ the Friedmann constraint (11) tends to the form of general relativity if (c) $\frac{1}{(2\omega(x_*)+3)^2} \frac{d\omega}{dx}\Big|_{x=x_*} \neq 0$. It must be also emphasized here that the process of taking the Taylor expansion (12) hinges on the assumption that (d) $\frac{1}{2\omega(x)+3}$ is differentiable (derivatives do not diverge) at x_* . In this context one may also ask when the full set of equations (6)-(9) attains the form of general relativity. It is easy to see that besides (a)-(d) one must also impose

$$\frac{1}{2\omega(x)+3} \frac{d\omega}{dx} y^2 = \frac{1}{(2\omega(x_*)+3)^2} \frac{d\omega}{dx} ((2\omega(x)+3)y^2) \rightarrow 0, \quad (15)$$

but the latter is automatically satisfied if (c) holds, due to (12), (14). Therefore we may tentatively call the conditions (a)-(d) ‘the general relativity limit of scalar-tensor flat FLRW cosmology’.

It is interesting to compare the cosmological GR limit to the GR limit obtained from PPN, which characterizes the slow motion approximation in a centrally symmetric gravitational field. Although the mathematical assumptions underlying the PPN formalism are clearly different from our cosmological reasoning above, we may still ask whether the results of both schemes agree with each other. In the context of PPN it is well established that the solutions of scalar-tensor theory approach those of general relativity when [34]

$$\frac{1}{2\omega(x) + 3} \rightarrow 0, \quad \frac{1}{(2\omega(x) + 3)^3} \frac{d\omega}{dx} \rightarrow 0. \quad (16)$$

Comparison shows that the cosmological conditions (a)-(d) are marginally stricter than the PPN condition (16), since (a), (c), (d) imply that (16) is satisfied, but (16) does not necessarily guarantee that (c) or (d) holds.

Let us also note that there is also another special case x_\bullet , realized at

$$\rho = 0, \quad y = 0, \quad 2V(x_\bullet) - x_\bullet \left. \frac{dV(x)}{dx} \right|_{x_\bullet} = 0, \quad (17)$$

when the cosmological equations (6)-(9) relax to those of general relativity featuring de Sitter evolution. However, as the value of $\omega(x_\bullet)$ is not fixed by the condition (17), this case does not conform with the GR limit of PPN. Therefore, even when the limits (a)-(d) and (17) can be cosmologically indistinguishable, Solar System observations in the PPN framework can in principle reveal which of the two is actually realized. (In this paper when using the phrase ‘the GR limit of STT’ we mean the conditions (a)-(d), as these take the STT cosmological equations to those of general relativity and also guarantee that the PPN condition is satisfied. But note that some authors, e.g. Refs. [18, 19] have not necessarily used the same definition.)

The general relativity limit of STT is purely given in terms of x and y . In the following we extract from the full dynamical system (6)-(9) an independent subsystem for $\{x, y\}$, find its fixed points and check whether the limit of general relativity matches to an attractive fixed point. But before, some general remarks about the full phase space are in order.

3 Phase space

In the four phase space dimensions $\{\Psi \equiv x, \dot{\Psi} \equiv y, H, \rho\}$ the physical trajectories (orbits of solutions) are those which satisfy the Friedmann constraint (2), i.e. which lie on the 3-surface

$$\mathcal{F} : F(x, y, H, \rho) \equiv H^2 + H \frac{y}{x} - \frac{y^2}{6x^2} \omega(x) - \frac{\kappa^2 \rho}{3x} - \frac{\kappa^2 V(x)}{3x} = 0. \quad (18)$$

It can be readily checked that the trajectories' tangent vector, $T^i = (\dot{x}, \dot{y}, \dot{H}, \dot{\rho})$, given by (6)-(9), is perpendicular to the normal of the Friedmann surface,

$$\nabla_i F \cdot T^i \Big|_{\mathcal{F}} = 0, \quad (19)$$

and therefore the system automatically obeys the Friedmann constraint, as the trajectories on the surface \mathcal{F} never leave it.

In principle the geometry of the Friedmann 3-surface in the 4-dimensional phase space is rather complicated to visualize, but a few general characteristics can still be given. We may write Eq. (18) as

$$\frac{\left(H + \frac{y}{2x}\right)^2}{\frac{\kappa^2(\rho+V)}{3x}} - \frac{y^2}{\frac{4\kappa^2x(\rho+V)}{2\omega+3}} = 1, \quad (20)$$

which for fixed ρ and x can be recognized as describing familiar conic sections: 1) for $\rho+V > 0$, $2\omega + 3 > 0$ a hyperbola on the $(H + \frac{y}{2x}, y)$ plane, 2) for $\rho + V > 0$, $2\omega + 3 < 0$ an ellipse also on the $(H + \frac{y}{2x}, y)$ plane, while 3) for $\rho + V < 0$, $2\omega + 3 > 0$ a hyperbola on the $(y, H + \frac{y}{2x})$ plane. The case 4) $\rho + V < 0$, $2\omega + 3 < 0$ is not realized as real solutions are absent. This result establishes that the intersection of the Friedmann 3-surface with the (fixed ρ , fixed x) 2-plane is constituted in either one piece (ellipse) or two pieces (hyperbola). Thus in case 1) the allowed phase space is divided into two separate regions, the ‘‘upper’’ region where $H + \frac{y}{2x} > 0$ and the ‘‘lower’’ region where $H + \frac{y}{2x} < 0$, and there is no way the trajectories can travel from one region to another. In case 2) these two regions meet along a 2-surface where $H + \frac{y}{2x} = 0$, and the trajectories can in principle cross from one region to another. In case 3) there are again two separate parts, now characterized by $y > 0$ and $y < 0$, respectively. At first it may be difficult find a direct physical interpretation for the quantity $H + \frac{y}{2x}$ that characterizes the ‘‘upper’’ and ‘‘lower’’ region in cases 1) and 2), but it turns out that this combination is equal to the Hubble parameter in the Einstein frame, see Eq. (39), and thus the ‘‘upper’’ region corresponds to universes which expand in the Einstein frame, while the ‘‘lower’’ region has universes which contract in the Einstein frame.

Related information can be also established by another approach. We may solve the Friedmann constraint for H , Eq. (11), and then the condition for all variables to be real valued imposes an inequality

$$(2\omega(x) + 3) \frac{y^2}{12x^2} + \frac{\kappa^2(\rho + V(x))}{3x} \geq 0. \quad (21)$$

In terms of physics this inequality can be interpreted as a restriction on the allowed values of y (see Table 1). There is no restriction in case 1), while the case 4) $\rho + V < 0$, $2\omega + 3 < 0$ is completely ruled out since no real solutions compatible with the Friedmann constraint exist in this case. Similarly, solving the Friedmann constraint for y leads to another inequality,

$$\frac{x^2}{\omega^2(x)} \left((2\omega(x) + 3)H^2 - \frac{2\kappa^2\omega(x)}{3x}(\rho + V(x)) \right) \geq 0, \quad (22)$$

		Allowed range of ω	Allowed range of $\dot{\Psi}$	Allowed range of H
1a)	$\rho + V \geq 0$	$0 \leq \omega \leq \infty$	$0 \leq \dot{\Psi}^2 \leq \infty$	$\frac{2\kappa^2\omega(\rho+V)}{3\Psi(2\omega+3)} \leq H^2 \leq \infty$
1b)	$\rho + V \geq 0$	$-\frac{3}{2} \leq \omega \leq 0$	$0 \leq \dot{\Psi}^2 \leq \infty$	$0 \leq H^2 \leq \infty$
2)	$\rho + V > 0$	$-\infty \leq \omega \leq -\frac{3}{2}$	$0 \leq \dot{\Psi}^2 \leq \frac{4\kappa^2(\rho+V)\Psi}{ 2\omega+3 }$	$0 \leq H^2 \leq \frac{2\kappa^2\omega(\rho+V)}{3\Psi(2\omega+3)}$
3a)	$\rho + V \leq 0$	$0 \leq \omega \leq \infty$	$\frac{4\kappa^2 \rho+V \Psi}{2\omega+3} \leq \dot{\Psi}^2 \leq \infty$	$0 \leq H^2 \leq \infty$
3b)	$\rho + V \leq 0$	$-\frac{3}{2} \leq \omega \leq 0$	$\frac{4\kappa^2 \rho+V \Psi}{2\omega+3} \leq \dot{\Psi}^2 \leq \infty$	$\frac{2\kappa^2\omega(\rho+V)}{3\Psi(2\omega+3)} \leq H^2 \leq \infty$
4)	$\rho + V < 0$	$-\infty < \omega < -\frac{3}{2}$	-	-

Table 1: Constraints from the Friedmann equation on the values of $\dot{\Psi} \equiv y$ (21) and H (22).

which can be interpreted as a restriction on the allowed values of H (given also in Table 1). Analogously, once $\omega(x)$ and $V(x)$ are specified, we may get a third inequality from solving the Friedmann constraint for x as well.

In terms of the phase space geometry the inequality (21) is saturated on a cylindrical 3-surface

$$\mathcal{B}_H : B_H(x, y, H, \rho) \equiv (2\omega(x) + 3) \frac{y^2}{12x^2} + \frac{\kappa^2(\rho + V(x))}{3x} = 0, \quad (23)$$

which is parallel to the H axis. In cases 2) and 3) it bounds the extent of the Friedmann surface (18) in the x, y, ρ directions, i.e., when we project the Friedmann surface along the H direction to the (x, y, ρ) 3-plane, the projection lies within the bounds set by \mathcal{B}_H . In case 1) the projection covers the entire (x, y, ρ) 3-plane. Correspondingly, the inequality (22) is saturated on the 3-surface

$$\mathcal{B}_{\dot{\Psi}} : B_{\dot{\Psi}}(x, y, H, \rho) \equiv \frac{x^2}{\omega^2(x)} \left((2\omega(x) + 3)H^2 - \frac{2\kappa^2\omega(x)}{3x}(\rho + V(x)) \right) = 0, \quad (24)$$

which is parallel to the y axis and bounds the extent of the Friedmann surface in the x, H, ρ directions.

In cases 2) and 3) the Friedmann 3-surface \mathcal{F} tangentially touches the cylindrical bounding 3-surface \mathcal{B}_H along a 2-surface defined by the union $\mathcal{F} \cup \mathcal{B}_H$. The touching is tangential,

$$\nabla_i B_H \cdot T^i \Big|_{\mathcal{F} \cup \mathcal{B}_H} = 0, \quad (25)$$

as the trajectories can not go through \mathcal{B}_H to the unphysical region. By substituting the condition (23) into the constraint equation (18) we see that on the 2-surface $\mathcal{F} \cup \mathcal{B}_H$ the quantity $H + \frac{y}{2x}$ vanishes, hence $\mathcal{F} \cup \mathcal{B}_H$ joins the above defined ‘‘upper’’ and ‘‘lower’’ regions of the Friedmann surface. We may ask, again relevant in cases 2) and 3) only, whether the

trajectories do cross between these two regions, i.e. whether they do pass through $\mathcal{F} \cup \mathcal{B}_H$. For this purpose let us introduce another 3-surface

$$\bar{\mathcal{B}}_H : \bar{B}_H(x, y, H, \rho) \equiv H + \frac{y}{2x} = 0, \quad (26)$$

distinct from \mathcal{F} and \mathcal{B}_H , but with the property that its intersection with the Friedmann surface coincides with the union of \mathcal{F} and \mathcal{B}_H , i.e., $\mathcal{F} \cup \bar{\mathcal{B}}_H = \mathcal{F} \cup \mathcal{B}_H = \mathcal{B}_H \cup \bar{\mathcal{B}}_H$. From the scalar product

$$\nabla_i \bar{B}_H \cdot T^i \Big|_{\mathcal{F} \cup \bar{\mathcal{B}}_H} = \frac{\kappa^2}{2x} ((1-w)\rho + 2V) \quad (27)$$

it follows that the trajectories pass through this intersection from “lower” region where $H + \frac{y}{2x} < 0$ to the “upper” region where $H + \frac{y}{2x} > 0$ if $((1-w)\rho + 2V)|_{\mathcal{F} \cup \bar{\mathcal{B}}_H} > 0$ and in the reverse direction if $((1-w)\rho + 2V)|_{\mathcal{F} \cup \bar{\mathcal{B}}_H} < 0$. Only if $w = 1$ and $V|_{\mathcal{F} \cup \bar{\mathcal{B}}_H} = 0$ do the trajectories, which are in the subspace $\mathcal{F} \cup \bar{\mathcal{B}}_H$, remain there in their entirety, and thus block the passage between the “upper” and “lower” regions.

In the next two sections we study the asymptotic behavior of solutions by finding the fixed points and their properties. Since the energy densities of different types of matter and the potential $V(\Psi)$ scale differently under the change of the scale factor of the Universe, one is justified to consider different regimes separately, specified by the dominant component.

4 Fixed points for potential domination ($V \not\equiv 0$, $\rho \equiv 0$)

In the limit of vanishing matter density the phase space shrinks to three dimensions $\{x \equiv \Psi, y \equiv \dot{\Psi}, H\}$, where the Friedmann constraint restrains the physical trajectories to lie on a two-dimensional surface \mathcal{F} . We may solve the Friedmann constraint for H , as (11), substitute it into Eq. (7), and thus in effect reduce the system 2-dimensional:

$$\begin{cases} \dot{x} &= y \\ \dot{y} &= \left(\frac{3}{2x} - \frac{1}{2\omega(x)+3} \frac{d\omega}{dx} \right) y^2 \underset{(-)}{\overset{(+)}{}} \frac{1}{2x} \sqrt{3(2\omega(x)+3)y^2 + 12\kappa^2 x V(x)} y + \frac{2\kappa^2}{2\omega(x)+3} \left(2V(x) - x \frac{dV}{dx} \right). \end{cases} \quad (28)$$

This constitutes a projection of the trajectories on the original two-dimensional constraint surface in (x, y, H) to the (x, y) plane. The projection yields two “sheets”: the “upper sheet” marked by the $-$ sign, and the “lower sheet” marked by the $\overset{(+)}{}$ sign in Eq. (28). In three dimensions the former corresponds to the “upper” region where $H + \frac{y}{2x} > 0$, while the latter to the “lower” region where $H + \frac{y}{2x} < 0$.

The consideration of only the variables $\{x, y\}$ and Eqs. (28) is in principle sufficient to follow the dynamics as the value of H can at each point be computed from the constraint (11). The only complication arises in cases 2) and 3) along the boundary $y^2 = \frac{4\kappa^2 x |V(x)|}{|2\omega(x)+3|}$ which marks the extent of the (x, y) -plane accessible for physical trajectories. In three dimensions

Condition	Eigenvalues
Ψ_{\bullet} $\frac{dV}{d\Psi}\Big _{\Psi_{\bullet}} - 2V(\Psi_{\bullet}) = 0$	$\begin{matrix} + \\ - \end{matrix} \left[-\sqrt{\frac{3\kappa^2 V}{4\Psi}} \pm \sqrt{\frac{\kappa^2}{2\omega+3} \left((6\omega+25)\frac{V}{4\Psi} - 2\Psi\frac{d^2V}{d\Psi^2} \right)} \right]_{\Psi_{\bullet}}$
Ψ_{\star} $\frac{1}{2\omega(\Psi_{\star})+3} = 0, \frac{1}{(2\omega(\Psi_{\star})+3)^2} \frac{d\omega}{d\Psi} \neq 0$	$\begin{matrix} + \\ - \end{matrix} \left[-\sqrt{\frac{3\kappa^2 V}{4\Psi}} \pm \sqrt{\frac{4\kappa^2}{(2\omega+3)^2} \frac{d\omega}{d\Psi} \left(\Psi\frac{dV}{d\Psi} - 2V \right) + \frac{3\kappa^2 V}{4\Psi}} \right]_{\Psi_{\star}}$

Table 2: Fixed points and their eigenvalues for the $V \neq 0, \rho \equiv 0$ case.

this boundary corresponds to the border $\mathcal{F} \cup \mathcal{B}_H$ where $H + \frac{y}{2x} = 0$ and the “upper” and “lower” regions meet. From the discussion around Eq. (27) we know that with the exception of some special cases the trajectories do traverse from one region to another, and thus in the two-dimensional projection picture must change the “sheet”. However, along the boundary the Friedmann surface is positioned perpendicularly to the (x, y) -plane and the projection (28) is then unable to encode the full dynamics of the system. Therefore with Eq. (28) it is possible to follow a trajectory on one “sheet” forwards until it reaches the boundary or backwards until it starts from the boundary, while the step of changing the sheet remains to be accounted by relying on the full system (6)-(9). Still, the system (28) is adequate for finding and describing the fixed points, at least as long as the prospective fixed points do not reside on the border of the two “sheets”.

Standard procedure reveals that the dynamical system (28) is endowed with two fixed points, Table 2 lists their conditions and eigenvalues. The first fixed point Ψ_{\bullet} satisfies

$$\frac{dV}{d\Psi}\Big|_{\Psi_{\bullet}} - 2V(\Psi_{\bullet}) = 0, \quad (29)$$

which matches the second limit (17), discussed in Sec. 2. It is rather surprising to note that a local extremum of the potential, $\frac{dV}{d\Psi} = 0$, does provide a fixed point only if the value of the potential vanishes at this point, $V(\Psi_{\bullet}) = 0$. In the latter case the eigenvalues tell that if this extremum is a maximum, $\frac{d^2V}{d\Psi^2} < 0$, the nature of this point is saddle, while a local minimum, $\frac{d^2V}{d\Psi^2} > 0$, is non-hyperbolic. But generally local minima with non-vanishing value of the potential do not figure as fixed points, while at the same time it is possible to have a fixed point residing on an arbitrary steep slope of the potential. This puzzling feature, however, becomes more meaningful when translated into the Einstein frame. As explained in Sec. 6 the condition (29) gives a local extremum of the Einstein frame potential.

The second fixed point Ψ_{\star} satisfies

$$\frac{1}{2\omega(\Psi_{\star})+3} = 0, \quad \frac{1}{(2\omega(\Psi_{\star})+3)^2} \frac{d\omega}{d\Psi}\Big|_{\Psi=\Psi_{\star}} \neq 0, \quad (30)$$

i.e. exactly the same conditions (a)-(d) as the limit of general relativity for flat FLRW STT cosmology, discussed in the end of Sec. 2. Again, the eigenvalues are listed in Table

2. In particular we see that on the “upper” sheet this point is an attractor if $V > 0$ and $\frac{4\kappa^2}{(2\omega+3)^2} \frac{d\omega}{d\Psi} \left(\Psi \frac{dV}{d\Psi} - 2V \right) < 0$, while on the “lower” sheet it can not be an attractor at all. (In principle it is also possible that the points Ψ_\bullet and Ψ_\star coincide. Yet, the properties of such a combined point are difficult to determine without knowing the exact form of ω and V .)

From Eq. (11) it is straightforward to compute that the values of H corresponding to the fixed points Ψ_\bullet and Ψ_\star are $H_\bullet = \binom{+}{-} \sqrt{\frac{\kappa^2 V(\Psi_\bullet)}{3\Psi_\bullet}}$ and $H_\star = \binom{+}{-} \sqrt{\frac{\kappa^2 V(\Psi_\star)}{3\Psi_\star}}$, respectively. The result, which mimics de Sitter evolution in general relativity, was expected, since we saw in Sec. 2 that under the fixed point conditions (29) and (30) the full STT equations (6)-(8) reduce to the equations of general relativity.

So, having a model of STT with given $\omega(\Psi)$ and $V(\Psi)$, one has to solve the conditions (29) and (30) to find the values of Ψ where fixed points occur. To determine the nature of these points it is necessary to compute the eigenvalues at these points, possibly using an appropriate limiting procedure. For the benefit of the reader, may we recall that when both eigenvalues are real and negative then we have a stable node (attractor), while real and positive eigenvalues indicate an unstable node (repeller). Complex eigenvalues with a negative real part give a stable focus (spiralling attractor), while a positive real part indicates an unstable focus. One positive and one negative real eigenvalue occur with a saddle point, but if the real part vanishes, the point is classified as non-hyperbolic and linear stability analysis is not enough to determine the behaviour of solutions around it.

As an illustration let us consider an example

$$\omega(\Psi) = \frac{3\Psi}{2(1-\Psi)}, \quad V(\Psi) = -2(\Psi - 0.2)^3 + 3(\Psi - 0.2)^2, \quad (31)$$

chosen to demonstrate some typical features that may crop up in a generic scalar-tensor theory. The shape of ω and V , along with the phase portraits are shown on Fig. 1. To briefly go through the main features let us first recall that while the phase space is 3-dimensional $(\Psi, \dot{\Psi}, H)$ the physical trajectories lie on the 2-dimensional Friedmann surface which is comprised of two sheets. The domain $\Psi \in (0, 1]$ belongs to case 1a) of Table 1, meaning the values of $\dot{\Psi}$ are not limited, and the “upper” and “lower” sheets are separate. On the other hand, the domain $\Psi \in [1, 1.7]$ belongs to the case 2), where the values of $\dot{\Psi}$ are limited and the “upper” and “lower” sheet meet along the $H + \frac{\dot{\Psi}}{2\Psi} = 0$ line. Finally, the domain $\Psi \in (1.7, \infty)$ falls under the case 4) where the Friedmann constraint does not have any real solutions.

There are three fixed points coming in two sets, one set for the “upper” and another for the “lower” sheet. Two of the fixed points satisfy the condition (29) and happen to have the same corresponding nature on both sheets: the point at $\Psi_\bullet = 0.2$ (where $V = 0$) is non-hyperbolic, while the other point at $\Psi_\bullet = 0.73$ is a saddle. The third fixed point $\Psi_\star = 1$ satisfies (30) and is an attractor on the “upper” sheet, but a repeller on the “lower” sheet. Fig. 1 (up, right) illustrates how the trajectories in the $\Psi \in [1, 1.7]$ domain start at the “lower” sheet repeller Ψ_\star , cross over to the “upper” sheet, and end up at the “upper” sheet attractor Ψ_\star . This behavior

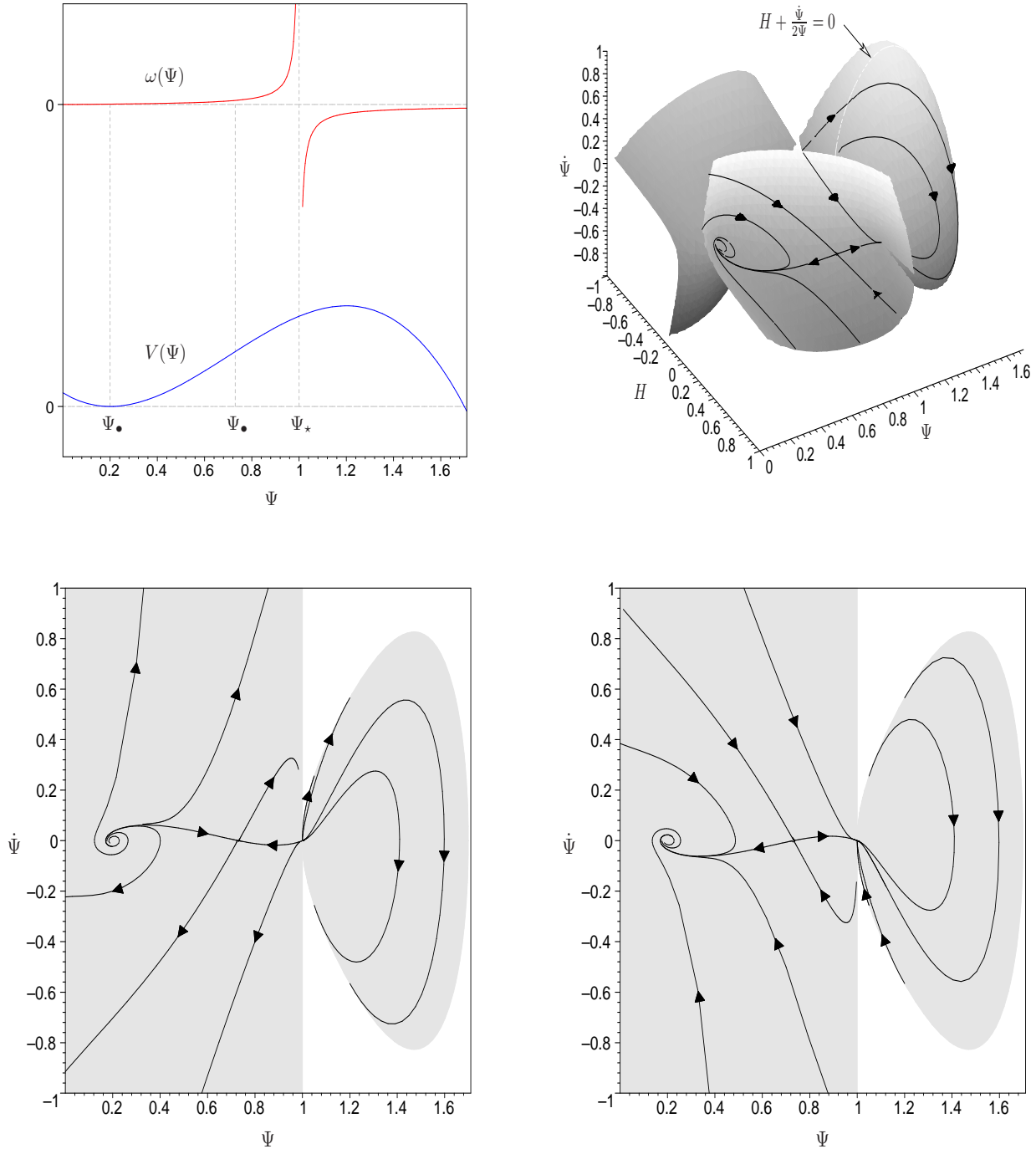


Figure 1: Illustration to the example (31) described in the text: the shape of ω and V (up, left); 3-dimensional phase space with two sheets where the physical trajectories reside (up, right); 2-dimensional projection of the “lower” sheet (down, left), and “upper” sheet (down, right).

is reflected on the projection, which shows the “lower” sheet trajectories (Fig. 1, down, left) running to the boundary in order to just emerge on the “upper” sheet boundary (down, right).

5 Fixed points for matter domination ($V \equiv 0$, $\rho \neq 0$)

In the case of cosmological matter ($\rho > 0$) and vanishing scalar potential the Friedmann constraint restricts the solutions onto a three-dimensional surface in four phase space dimensions ($x \equiv \Psi, y \equiv \dot{\Psi}, H, \rho$). However, the system is amenable to a change of the time variable, first used by Damour and Nordtvedt [12] in the Einstein frame, that allows to combine the field equations into a dynamical equation for the scalar field which does not manifestly contain the scale factor or matter density. In the Jordan frame this amounts to defining a new time variable p [15]

$$dp = h_c dt \equiv \left| H + \frac{\dot{\Psi}}{2\Psi} \right| dt. \quad (32)$$

Then from Eqs. (2)–(4) the following “master” equation for the scalar field can be derived [15, 24]:

$$\begin{aligned} \Psi'' \begin{matrix} - \\ (+) \end{matrix} \frac{(2\omega(\Psi) + 3)(1 - w)}{8\Psi^2} \Psi'^3 - \left(\frac{3(1 + w)}{4\Psi} - \frac{1}{2\omega(\Psi) + 3} \frac{d\omega(\Psi)}{d\Psi} \right) \Psi'^2 \\ + \begin{matrix} + \\ (-) \end{matrix} \frac{3(1 - w)}{2} \Psi' - \frac{3(1 - 3w)}{(2\omega(\Psi) + 3)} \Psi = 0, \end{aligned} \quad (33)$$

where primes denote the derivatives with respect to p . The transformation of the time coordinate (32) managed to align the phase space trajectories in a way that made a projection into two dimensions possible. Like in the previous section the upper signs in Eq. (33) correspond to the “upper” sheet where the quantity $H + \frac{\dot{\Psi}}{2\Psi}$ is positive, while the lower signs to the “lower” sheet where the quantity $H + \frac{\dot{\Psi}}{2\Psi}$ is negative.

The “master” equation can be relied on as long as $h_c = |H + \frac{\dot{\Psi}}{2\Psi}|$ is finite. At $\Psi = 0$ the quantity h_c diverges making the t -time to stop with respect to the p -time. Hence all t -time trajectories with finite $\dot{\Psi}$ get mapped to $\Psi' = 0$, giving a false impression of a fixed point there. However, in Sec. 2 we concluded that $\Psi = 0$ comes with a space-time singularity and exclude it from present analysis.

The other problematic points can be discussed by noticing that in terms of the new time variable p the Friedmann constraint (2) can be written as

$$h_c^2 = \frac{\kappa^2 \rho}{3\Psi \left(1 - \frac{(2\omega(\Psi) + 3) \Psi'^2}{12\Psi^2} \right)}. \quad (34)$$

To keep h_c real, the right hand side of Eq. (34) must be nonnegative, thus constraining the dynamically allowed regions of the two-dimensional phase space (Ψ, Ψ') of the scalar field (see

		Allowed range of $\dot{\Psi}$	Allowed range of Ψ'
1)	$\rho > 0 \quad 2\omega + 3 > 0$	$0 \leq \dot{\Psi}^2 < \infty$	$0 \leq \Psi'^2 < \frac{12\Psi^2}{2\omega+3}$
2)	$\rho > 0 \quad 2\omega + 3 \leq 0$	$0 \leq \dot{\Psi}^2 \leq \frac{4\kappa^2 \rho \Psi}{ 2\omega+3 }$	$0 \leq \Psi'^2 < \infty$

Table 3: Constraints from the Friedmann equation on the scalar field phase space in t -time from Eq. (21) and p -time from Eq. (34).

Table 3). At the boundaries of the allowed regions the time transformation (32) fails to be meaningful. In case 1) the boundary

$$\Psi'^2 = \frac{12\Psi^2}{2\omega(\Psi) + 3} \quad (35)$$

is characterized by t -time stopping with respect to p -time, and as a result finite Ψ' corresponds to $\dot{\Psi}^2 \rightarrow \infty$. Considering t -time to be physical permits us to exclude this boundary from analysis on physical grounds. In case 2) the limit $\Psi' \rightarrow \infty$ corresponds to finite $\dot{\Psi}$, since p -time stops with respect to t -time. As $h_c = |H + \frac{\dot{\Psi}}{2\Psi}| = 0$ the latter boundary also marks the joint of the “upper” and “lower” sheets. Therefore, in p -time it is not possible to follow the passage of trajectories from one sheet to another, but as the general considerations presented after Eq. (27) inform us, the trajectories do pass from the “lower” to “upper” sheet if $w < 1$ and vice versa if $w > 1$, while in the $w = 1$ case the passage is blocked by trajectories which lie entirely on this boundary. Despite the shortcoming that the two-dimensional “master” equation (33) is not able to capture all the details of the full dynamics in the four-dimensional phase space, we can still use it for finding the fixed points for Ψ as long as the fixed points do not reside on the problematic boundary.

Let us consider the cosmological matter behaving like dust ($w = 0$) first. Introducing $\Psi = x$, $\Psi' = z$ enables to write Eq. (33) as a dynamical system:

$$\begin{cases} x' &= z \\ z' &= \begin{matrix} + \\ (-) \end{matrix} \frac{2\omega(x)+3}{8x^2} z^3 + \frac{6\omega(x)+9-4x\frac{d\omega(x)}{dx}}{4x(2\omega(x)+3)} z^2 \begin{matrix} - \\ (+) \end{matrix} \frac{3}{2} z + \frac{3x}{2\omega(x)+3}. \end{cases} \quad (36)$$

An argument completely analogous to the one put forth for Eq. (12), reveals a single fixed point, satisfying the conditions (a)-(d) dubbed as the limit of general relativity for flat FLRW STT in Sec. 2. The corresponding eigenvalues, to be evaluated at the fixed point coordinate, are given in Table 4. In particular, this point is an attractor on the “upper” sheet if $\frac{d\omega}{d\Psi} > 0$, while on the “lower” sheet attractor behavior is not possible.

To complete the analysis it is important to verify that the fixed point just found in the p -time does indeed correspond to a fixed point in the cosmological t -time. But since we have

Case	Fixed point	Condition	Eigenvalues
$w = 0$	Ψ_*	$\frac{1}{2\omega(\Psi_*)+3} = 0, \frac{1}{(2\omega(\Psi_*)+3)^2} \frac{d\omega}{d\Psi} \neq 0$	$\begin{matrix} + \\ (-) \end{matrix} \left[-\frac{3}{4} \pm \frac{3}{4} \sqrt{1 - \frac{32}{3} \frac{\Psi}{(2\omega+3)^2} \frac{d\omega}{d\Psi}} \right]_{\Psi_*}$
$w = \frac{1}{3}$	none		

Table 4: Fixed points and their eigenvalues for the $\rho \neq 0, V \equiv 0$ case.

excluded the boundary (35) and consider only the trajectories with finite h_c , it is immediate that $\Psi' = 0$ implies $\dot{\Psi} = 0$, due to (32). From Eq. (11) now it also follows that at the fixed point the evolution of the universe obeys the usual Friedmann equation from general relativity, $H_*^2 = \frac{\kappa^2 \rho}{3\Psi_*}$. This is expected, as the fixed point conditions were identical to the general relativity limit.

The dynamical system in the radiation dominated regime ($w = \frac{1}{3}$) reads

$$\begin{cases} x' = z \\ z' = \begin{matrix} + \\ (-) \end{matrix} \frac{2\omega(x)+3}{12x^2} z^3 + \frac{8\omega(x)+12-4x\frac{d\omega(x)}{dx}}{4x(2\omega(x)+3)} z^2 \begin{matrix} - \\ + \end{matrix} z. \end{cases} \quad (37)$$

There are no fixed points. For small values of $\Psi' = z$ the system is ruled by friction on the “upper” sheet, as the $-$ sign of the dominating term forces the vector flow to converge to the $z' = 0$ axis. On the “lower” sheet, the the effect is the opposite (anti-friction).

6 Discussion

A lot of work in FLRW scalar-tensor cosmology has been performed in the Einstein frame which is obtained from the Jordan frame by two transformations [28, 30]: (1) a conformal transformation of the metric $\tilde{g}_{\mu\nu}^{(E)} = \Psi g_{\mu\nu}^{(J)}$, followed by a coordinate transformation to keep the FLRW form of the line element, $d\tilde{t} = \sqrt{\Psi} dt$, and (2) a redefinition of the scalar field

$$(2\omega(\Psi) + 3)(d\Psi)^2 = 4\Psi^2(d\phi)^2. \quad (38)$$

The two frames are mathematically equivalent and hence also physically equivalent, as long as these two transformations are regular [28, 29, 3, 30, 31]. Both transformations become singular in the limit $\Psi \rightarrow 0$, while the latter transformation is also singular in the limit $2\omega(\Psi) + 3 \rightarrow 0$. These singularities were scrutinized in Refs. [23, 32, 33] with the conclusion that both frames retain equivalence in the sense that in both frames the Cauchy problem fails to be well posed in these limits. In Sec. 2 we also observed in passing that approaching these two limits generically leads to a space-time singularity in the Jordan frame.

The transformation (38) happens to be singular in the limit of general relativity, $\frac{1}{2\omega(\Psi)+3} \rightarrow 0$, as well. Ref. [20] also gives explicit examples of coupling functions $\omega(\Psi)$ where the phase

portraits for regions containing the GR limit are qualitatively inequivalent in the two frames. Therefore it is not guaranteed that the properties of the Ψ_* fixed point which resides at the general relativity limit are exactly the same in the Einstein frame. To actually compare the two frames in this respect, it would be necessary to perform a similar fixed point analysis in the Einstein frame.

The other fixed point, Ψ_\bullet , however, should have the same properties in the Einstein frame as in the Jordan frame, as long as it resides in the region where the transformations between the two frames are regular.

The conformal transformation relates the Hubble parameters in the two frames as

$$\tilde{H}_E = \frac{1}{\sqrt{\Psi}} \left(H_J + \frac{\dot{\Psi}}{2\Psi} \right). \quad (39)$$

Therefore the sign of the quantity $H_J + \frac{\dot{\Psi}}{2\Psi}$ which in our Jordan frame analysis distinguished the “upper” and “lower” sheet of the Friedmann surface, has a clear interpretation in the Einstein frame as indicating the expanding or collapsing universe. Also, as the scalar potentials in the two frames are related by

$$V_E(\phi(\Psi)) = \frac{1}{\Psi^2} V_J(\Psi), \quad (40)$$

it follows that the fixed point Ψ_\bullet given by Eq. (29) indeed corresponds to the local extremum of V_E [27]:

$$\left. \frac{dV_E}{d\phi} \right|_{\phi(\Psi_\bullet)} = \frac{1}{\Psi_\bullet^3} \left[\left. \frac{dV}{d\Psi} \Psi - 2V \right]_{\Psi_\bullet} \left. \frac{d\Psi}{d\phi} \right|_{\Psi_\bullet} = 0. \quad (41)$$

Among the two types of fixed points we found, Ψ_\bullet and Ψ_* , it is the latter which deserves particular interest, since it satisfies the PPN limit of general relativity and good conformity with Solar System experiments is guaranteed. The existence of Ψ_* relies on the conditions (a)-(d) given in Sec. 2, while its nature (attractor or other) is determined by the eigenvalues listed in Tables 2 and 4. Previous phase space analyses performed for specific examples of coupling functions and potentials which have considered this point [24, 20] are in accord with our general results. Still, we may also attempt a comparison with relevant studies carried out by other methods.

Damour and Nordtvedt [12] argue that for large classes of coupling functions $\alpha^2(\phi) = \frac{1}{2\omega(\Psi)+3}$ solutions are driven to the value of scalar field where the coupling function α vanishes, the scalar field decouples and we are left with general relativity. Their investigations were performed in the Einstein frame using approximate late time solutions and their results are in qualitative agreement with our results: for radiative matter, there is no specific fixed point, for dust matter general relativity is a fixed point. For instance taking linear coupling, $\alpha(\phi) = K\phi$ with $K = \text{const} > 0$, in the matter dominated regime, they found that for $K < \frac{3}{8}$ the system exhibits damped behavior, while for $K > \frac{3}{8}$ the behavior is damped-oscillatory. In our analysis this can be compared to the Ψ_* fixed point. Plugging in the coupling to the eigenvalues in

Table 4 gives $-\frac{3}{4} \pm \frac{3}{4}(\sqrt{1 - \frac{16}{3}K})$, indicating a stable node (attractor) for $K < \frac{3}{16}$ and stable focus (spiralling attractor) for $K > \frac{3}{16}$. The slight difference in the numerical factor may reflect the difference between the frames, or perhaps can be attributed to the fact that in making the approximation Damour and Nordtvedt drop some terms in the scalar field equation.

Recently Barrow and Shaw [16] analysed the asymptotic behavior of homogeneous and isotropic cosmological solutions of general scalar-tensor theory containing a two-component perfect fluid: vacuum 'dark energy' ($p_0 = -\rho_0$, essentially a constant potential) and subdominant matter density. They demonstrate that if STT cosmology evolves toward the de Sitter limit at late time, then there exists an asymptotic value of the scalar field $\Psi_\infty \in (0, \infty)$ such that for $\Psi \rightarrow \Psi_\infty$ it holds that $\omega \rightarrow \infty$ and $\frac{1}{\omega^{2+\epsilon}} \frac{d\omega}{d\Psi} \rightarrow 0$ for any $\epsilon > 0$. In our analysis of Sec. 4 this can be compared to the solutions closing in on the fixed point Ψ_* yielding de Sitter expansion. The conditions for the existence of Ψ_* , (a) $\frac{1}{2\omega+3} \rightarrow 0$ and (c) $\frac{1}{(2\omega+3)^2} \frac{d\omega}{d\Psi} \Big|_{\Psi=\Psi_*} \neq 0$ are slightly stronger than the ones of Barrow and Shaw. Namely, if Ψ_* is identified with Ψ_∞ , then (a) and (c) imply the conditions given by Barrow and Shaw, but the reverse does not necessarily follow, since (c) may not be satisfied.

Finally let us note that scalar-tensor theory has some features which allow it to be seen as a simplistic toy model of the low energy effective actions derived from string/M-theory compactifications. Namely, the latter usually involve a number of scalar fields (moduli of the compactification) and some of these are coupled to the Ricci scalar in the Jordan/string frame description. For phenomenological reasons it is important to have the moduli stabilized at fixed values. Typical scenarios of string theory moduli stabilization involve generating a scalar potential whereby the moduli can stabilize at the minimum of the potential [35]. In our notation this parallels to invoking the fixed point Ψ_\bullet . However, it would be interesting to see whether the other fixed point, Ψ_* , occurring at the singularity of the scalar field kinetic term, can also be generalized for string theory compactifications and what role can it play in stabilizing the string theory moduli.

7 Conclusion

We have considered flat FLRW cosmological models in general scalar-tensor theories with arbitrary coupling function $\omega(\Psi)$ and scalar potential $V(\Psi)$ in the Jordan frame. Using the methods of dynamical systems we have described the general geometry of the phase space and found the scalar field fixed points in two distinct asymptotic regimes: potential domination ($V \neq 0, \rho \equiv 0$), and matter domination ($V \equiv 0, \rho \neq 0$). In nutshell there are two types of fixed points arising from different mechanisms: Ψ_\bullet from a condition on the potential (equalling the local extremum of the Einstein frame potential) and Ψ_* from the singularity of the scalar field kinetic term. Approaching both types of fixed points the cosmological equations coincide with those of general relativity, yielding de Sitter expansion in the potential domination case

and Friedmann evolution in the matter domination case. However, for the Solar System experiments in the PPN framework only the fixed points of Ψ_* type give predictions identical with those of general relativity. The nature of fixed points (attractor or otherwise) depends on the functional forms of $\omega(\Psi)$ and $V(\Psi)$ according to corresponding eigenvalues given in Tables 2 and 4. Therefore, in Jordan frame analysis, general relativity is an attractor for a large class of scalar-tensor models, but not for all.

Provided the transformation relating the Jordan and Einstein frame is regular, there is an exact correspondence between the two frames and the Jordan frame phase space results should carry over to the Einstein frame. This is the case for the fixed point Ψ_\bullet . However, as the transformation of the scalar field fails to be regular in the limit of general relativity, the properties of the Ψ_* fixed point may be altered in the Einstein frame. To establish whether or how the correspondence holds in this case calls for a separate matching investigation in the Einstein frame.

Acknowledgements

We are grateful to the anonymous referee for clarifying questions. This work was supported by the Estonian Science Foundation Grant No. 7185 and by Estonian Ministry for Education and Science Support Grant No. SF0180013s07. MS also acknowledges the Estonian Science Foundation Post-doctoral research grant No. JD131.

References

- [1] C. M. Will, *Theory and experiment in gravitational physics* (Cambridge University Press, Cambridge, 1981).
- [2] Y. Fujii and K. Maeda, *The scalar-tensor theory of gravitation* (Cambridge University Press, Cambridge, 2003).
- [3] V. Faraoni, *Cosmology in scalar-tensor gravity* (Kluwer Academic Publishers, Dordrecht, 2004).
- [4] M. T. Anderson, *Notices Amer. Math. Soc.* **51**, 184 (2004).
- [5] P. J. Steinhardt and F. S. Accetta, *Phys. Rev. Lett.* **64**, 2740 (1990); J. Garcia-Bellido and D. Wands, *Phys. Rev. D* **52**, 6739 (1995) [arXiv:gr-qc/9506050]; J. Garcia-Bellido and M. Quiros, *Phys. Lett. B* **243**, 45 (1990).
- [6] F. Perrotta, C. Baccigalupi, and S. Matarrese, *Phys. Rev. D* **61**, 023507 (1999) [arXiv:astro-ph/9906066]; N. Bartolo and M. Pietroni, *Phys. Rev. D* **61**, 023518 (1999) [arXiv:hep-ph/9908521]; G. Esposito-Farese and D. Polarski, *Phys. Rev. D* **63**,

- 063504 (2001) [arXiv:gr-qc/0009034]; B. Boisseau, G. Esposito-Farese, D. Polarski, and A. A. Starobinsky, Phys. Rev. Lett. **85**, 2236 (2000) [arXiv:gr-qc/0001066]; A. Riazuelo and J. P. Uzan, Phys. Rev. D **66**, 023525 (2002) [arXiv:astro-ph/0107386]. E. Elizalde, S. Nojiri, and S. D. Odintsov, Phys. Rev. D **70**, 043539 (2004) [arXiv:hep-th/0405034].
- [7] S. Capozziello, S. Nojiri, and S. D. Odintsov, Phys. Lett. B **634**, 93 (2006) [arXiv:hep-th/0512118]; R. Gannouji, D. Polarski, A. Ranquet, and A. A. Starobinsky, JCAP **0609**, 016 (2006) [arXiv:astro-ph/0606287]; S. Nesseris and L. Perivolaropoulos, Phys. Rev. D **75**, 023517 (2007) [arXiv:astro-ph/0611238]; S. Capozziello, S. Nesseris, and L. Perivolaropoulos, JCAP **0712**, 009 (2007) [arXiv:0705.3586 [astro-ph]]; M. Demianski, E. Piedipalumbo, C. Rubano, and P. Scudellaro, arXiv:0711.1043 [astro-ph]; G. Barenboim and J. Lykken, JCAP **0803**, 017 (2008) [arXiv:0711.3653 [astro-ph]].
- [8] G. Esposito-Farese, AIP Conf. Proc. **736**, 35 (2004) [arXiv:gr-qc/0409081]; T. Clifton, D. F. Mota, and J. D. Barrow, Mon. Not. Roy. Astron. Soc. **358**, 601 (2005) [arXiv:gr-qc/0406001]; Wei-Tou Ni, Int. J. Mod. Phys. D **14**, 901 (2005) [arXiv:gr-qc/0504116]; S. G. Turyshev, Annu. Rev. Nucl. Part. Sci. **58**, 207 (2008) [arXiv:0806.1731 [gr-qc]].
- [9] S. Tsujikawa, K. Uddin, S. Mizuno, R. Tavakol, and J. Yokoyama, Phys. Rev. D **77**, 103009 (2008) [arXiv:0803.1106 [astro-ph]].
- [10] J. D. Bekenstein and A. Meisels, Phys. Rev. D **18**, 4378 (1978).
- [11] T. Damour and K. Nordtvedt, Phys. Rev. Lett. **70**, 2217 (1993).
- [12] T. Damour and K. Nordtvedt, Phys. Rev. D **48**, 3436 (1993).
- [13] J.-M. Gérard and I. Mahara, Phys. Lett. B **346**, 35 (1995); A. Serna and J. M. Alimi, Phys. Rev. D **53**, 3074 (1996) [arXiv:astro-ph/9510139];
- [14] J. D. Barrow and J. P. Mimoso, Phys. Rev. D **50**, 3746 (1994); J. D. Barrow and P. Parsons, Phys. Rev. D **55**, 1906 (1997) [arXiv:gr-qc/9607072]; D. I. Santiago, D. Kalligas, and R. V. Wagoner, Phys. Rev. D **58**, 124005 (1998), [arXiv:gr-qc/9805044]; A. Navarro, A. Serna, and J. M. Alimi, Phys. Rev. D **59**, 124015 (1999) [arXiv:astro-ph/9903368]; J. M. Alimi and J. M. Fuzfa, arXiv:0804.4100 [astro-ph].
- [15] A. Serna, J. M. Alimi, and A. Navarro, Class. Quant. Grav. **19**, 857 (2002) [arXiv:gr-qc/0201049];
- [16] J. D. Barrow and D. J. Shaw, Class. Quant. Grav. **25**, 085012 (2008) [arXiv:0712.2190 [gr-qc]].

- [17] A. Billyard, A. Coley and J. Ibáñez, Phys. Rev. D **59**, 023507 (1998) [arXiv:gr-qc/9807055]; T. C. Charters, A. Nunes, and J. P. Mimoso, Class. Quant. Grav. **18**, 1703 (2001) [arXiv:gr-qc/0103060]; N. Agarwal and R. Bean, arXiv:0708.3967 [astro-ph].
- [18] J. P. Mimoso and A. M. Nunes, Phys. Lett. A **248**, 325 (1998).
- [19] S. Carloni, S. Capozziello, J. A. Leach, and P. K. S. Dunsby, Class. Quant. Grav. **25**, 035008 (2008) [arXiv:gr-qc/0701009].
- [20] L. Järv, P. Kuusk, and M. Saal, Phys. Rev. D **76**, 103506 (2007) [arXiv:0705.4644 [gr-qc]].
- [21] E. Gunzig, V. Faraoni, A. Figueiredo, T. M. Rocha and L. Brenig, Class. Quant. Grav. **17**, 1783 (2000); A. Figueiredo, T. M. Rocha Filho, E. Gunzig, L. Brenig and A. Saa, Int. J. Theor. Phys. **41**, 2037 (2002) [arXiv:gr-qc/0210090]; F. C. Carvalho and A. Saa, Phys. Rev. D **70**, 087302 (2004) [arXiv:astro-ph/0408013]; F. Finelli, A. Tronconi, and G. Venturi, Phys. Lett. B **659**, 466 (2008) [arXiv:0710.2741 [astro-ph]].
- [22] E. Gunzig, A. Saa, L. Brenig, V. Faraoni, T. M. Rocha Filho and A. Figueiredo, Phys. Rev. D **63**, 067301 (2001) [arXiv:gr-qc/0012085].
- [23] L. R. Abramo, L. Brenig, E. Gunzig and A. Saa, Int. J. Theor. Phys. **42**, 1145 (2003) [arXiv:gr-qc/0305008].
- [24] L. Järv, P. Kuusk, and M. Saal, Phys. Rev. D **75**, 023505 (2007) [arXiv:gr-qc/0608109].
- [25] V. Faraoni, Ann. Phys. (N.Y.) **317**, 366 (2005) [arXiv: gr-qc/0502015].
- [26] A. Burd and A. Coley, Phys. Lett. B **267**, 330 (1991).
- [27] V. Faraoni, M. N. Jensen, and S. A. Theuerkauf, Class. Quant. Grav. **23**, 4215 (2006) [arXiv:gr-qc/0605050].
- [28] R. H. Dicke, Phys. Rev. **125**, 2161 (1962).
- [29] S. Weinberg, *Gravitation and cosmology* (Wiley, New York, 1972).
- [30] E. E. Flanagan, Class. Quant. Grav. **21**, 3817 (2004) [arXiv:gr-qc/0403063].
- [31] V. Faraoni and S. Nadeau, Phys. Rev. D **75**, 023501 (2007) [arXiv:gr-qc/0612075].
- [32] V. Faraoni, Phys. Rev. D **70**, 047301 (2004) [arXiv:gr-qc/0403020].
- [33] V. Faraoni and N. Lanahan-Tremblay, arXiv:0808.1943 [gr-qc].

- [34] K. J. Nordtvedt, *Astrophys. J.* **161**, 1059 (1970).
- [35] S. Kachru, M. B. Schulz and S. Trivedi, *JHEP* **0310**, 007 (2003) [arXiv:hep-th/0201028]; V. Balasubramanian, P. Berglund, J. P. Conlon and F. Quevedo, *JHEP* **0503** 007 (2005) [arXiv:hep-th/0502058]; O. DeWolfe, A. Giryavets, S. Kachru and W. Taylor, *JHEP* **0507** 066 (2005) [arXiv:hep-th/0505160]; L. Järv, T. Mohaupt and F. Saueressig, *JCAP* **0402** 012 (2004) [arXiv:hep-th/0310174].